Analysis and Optimization of Passive Intermodulation in Microwave Coaxial Cavity Filters

In-Kui Cho, Jin Tae Kim, Myung Yung Jeong, Tae-Goo Choy, and Young Il Kang

We studied how the passive intermodulation (PIM) power arising in air cavity filters could be calculated and how the design of the filter could be optimized in order to reduce the amplitude of the PIM signal. To do this, using simulated results, we optimized the various parameters of a filter. PIM in an air cavity filter depends on the power dissipated in its cavities. A reduction of this power loss therefore decreases the PIM power in the air cavity filter. Our experimental results confirm that it is possible to design and produce air cavity filters that generate low PIM signals.

Manuscript received Nov. 15, 2001; revised Dec. 6, 2002.

In-Kui Cho (phone:+82 42 860 1242, e-mail: cho303@etri.re.kr), Jin Tae Kim (e-mail: myjinny@etri.re.kr), Myung Yung Jeong (e-mail: myjeong@etri.re.kr), Tae-Goo Choy (e-mail: tgchoy@etri.re.kr), and Young Il Kang (e-mail: yikang@etri.re.kr) are with Basic Research Laboratory, ETRI, Daejeon, Korea.

I. INTRODUCTION

The generation of passive intermodulation (PIM) signals, when two or more RF signals are impressed onto a transmission line or communication system, can limit the channel capacity [1]. PIM signals result from the non-linearity in the RF component's power response [2]. The components that can produce PIM signals are various types of wave-guide and coaxial structures, filters, combiners, and antennas [3]-[5]. PIM signals are extremely troublesome, since once they are generated, they cannot be compensated for, because they are generated beyond the receive-reject filter. The mechanisms for the generation of these PIM signals are known and can be grouped as signals involving contact non-linearity and signals involving material non-linearity [1].

Several researchers have been interested in the PIM problem. F. Arazm et al. [6], for example, presented information on the generation of intermodulation products arising from non-linearities at metal-to-metal contacts. They concentrated on PIM signals generated at the contact faces between both similar and dissimilar metals, which included copper, beryllium-copper, brass, and various other materials. B. Deats et al. [7] predicted the PIM produced by a cable assembly through PIM source modeling. J Wilcox et al. [8] calculated the intermodulation products arising from the thermal heating of coaxial cable walls. In practice, methods for suppressing PIM require high quality workmanship.

Our investigation considers the PIM signals produced by air cavity filters. This paper begins with a short review of the PIM problem for coaxial structure configurations and extends these ideas to discuss the PIM characteristics in an air cavity filter. We calculate the power dissipated in each resonator that makes up the air cavity filter, and in this way we can see which

resonator gives rise to the dominant PIM signal in the pass band. We then discuss the levels of PIM signals for various cavity sizes of a six-cavity filter and investigate whether we can minimize PIM signals by adjusting the inner radius of the cavity in the filter when the outer radius is fixed. Our study reveals the relationship between RF performance and the amount of PIM signal generated. Finally, to verify our design and predictions, we describe the manufacture and measurement of an experimental filter.

II. DESIGN AND MODELING

Because of the finite conductivity of metal, there always exists an RF energy loss in the metallic walls of a coaxial wave-guide in a volume defined approximately by the thickness of the skin depth. The cyclic variations of energy within this volume are followed instantaneously by a change in temperature. Since metallic conductivity depends linearly on temperature, $\sigma = \sigma_0(1-\gamma\Delta T)$, where σ is the metallic conductivity, γ is the coefficient of resistivity, and T is the temperature [8], it also has harmonic components that will produce wall currents at the PIM frequency. These phenomena are presented by energy conservation principles and energy conversion.

A study of PIM currents generated in coaxial walls is found in [8].

$$j_s(b,r) = \Lambda_b(r)e^{-3r/\delta}\sin(\omega t - \frac{r}{\delta} + \frac{\pi}{4}),$$

$$\text{where } \Lambda_b(r) = \frac{\gamma\sigma_0^{\,2}}{8c_p}\cdot\frac{5\omega_1-\omega_2}{\omega_1(\omega_2-\omega_1)}\cdot E_{1,z}^{\,2}(b)E_{2,z}(b)e^{-3r/\delta}\cdot\sin(\omega t - \frac{r}{\delta} + \frac{\pi}{4}), \quad (1)$$

where J_s is the PIM source current, b is the outer radius of coaxial cable, δ is the skin depth, ω is $2\omega_1-\omega_2$, and c_p is the specific heat.

These PIM source currents support PIM fields. In conclusion, the PIM power is equal to

$$\begin{aligned} P_{IM} &= \frac{c}{4}\frac{b^2}{\sqrt{\varepsilon}}\ln\frac{b}{a}H_{IM}^{\,2}(b) \\ &= \left(\frac{69}{128\pi}\right)^{1/2}\frac{c\omega_2}{8\pi\sigma}\frac{\gamma^2}{c_p^2}\left(1+\frac{b^3}{a^3}\right)^2\frac{\sqrt{\varepsilon}}{\left(\ln\frac{b}{a}\right)} \\ &\quad\cdot\left(\frac{5\omega_1-\omega_2}{\omega_2-\omega_1}\right)^2 H_1^4(b)H_2^2(b)z^2, \end{aligned} \quad (2)$$

where, c, a, and $H_1(b)$ are the velocity of light in free space, the inner radius of the coaxial cable, and the H-field of frequency ω_1 at the outer radius b, respectively. This PIM power can therefore relate to the two impressed powers, frequencies, material constants, and wave-guide structure.

To study the PIM problem for an air cavity filter consisting of several cavities, we investigated the transmission line resonators. In many microwave filter designs, a length of transmission line, terminating in either an open-circuit or a short-circuit, is often used as a resonator. Figure 1 illustrates a resonator made from a one-quarter wavelength short-circuit transmission line, together with its lumped element equivalent circuits [9], [10].

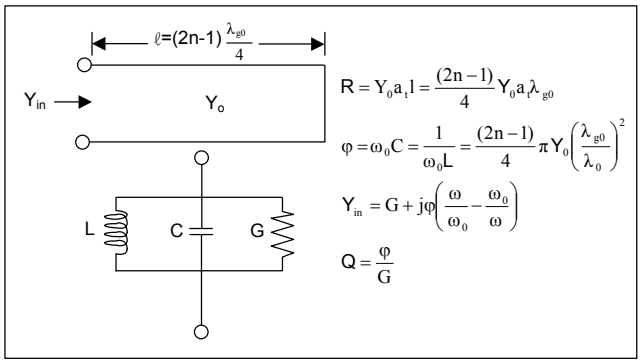

Fig. 1. A transmission line resonator with a short-circuit termination.

Here the transmission line admittance Y_0 is based on the transmission structure. For example, if it is a coaxial structure, the admittance is $\sqrt{C/L} = 2\pi/(\eta \ln b/a)$.

We can design the filter to be composed of transmission line resonators with short-circuit termination. Figure 2 shows an equivalent circuit for a six-resonator filter with a 947.5 MHz center frequency, 25 MHz bandwidth, and 0.01 dB ripple. This filter is built using a coaxial line resonator with an inner radius of 6 mm and an outer radius of 18 mm. Each resonator is represented as an RLC tank circuit, and these resonators are coupled together with j inverters [9].

III. SIMULATION OF PASSIVE INTERMODULATION

We simulated the circuit using the model in Fig. 2 and by circuit analysis calculated the voltages in each of the resonators for the six-cavity filter. The voltages in each of the resonators are shown in Fig. 3. The voltages in each resonator are symmetric with respect to the center frequency because the resonance frequencies of our individual resonators are symmetrically the same. We see that the voltages in resonator 2 and resonator 3 dominate at both the lower band edge and the upper band edge. These voltages in the resonators gave us a

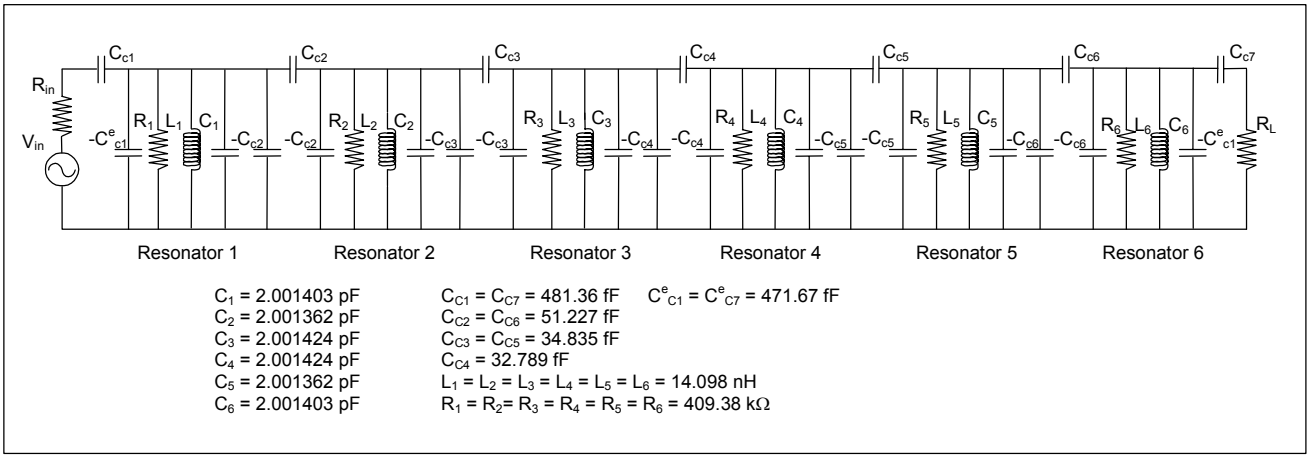

Fig. 2. The lumped-element model of a six-resonator filter.

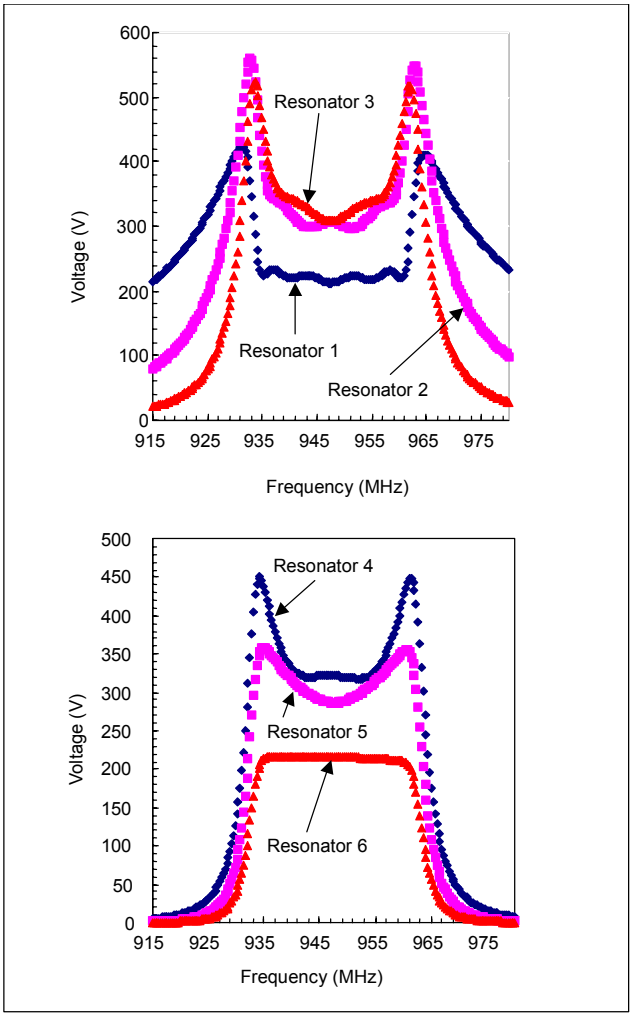

Fig. 3. Voltage versus frequency responses for each cavity resonator of the six-cavity filter.

hint about the contribution of the individual resonator to the power loss and PIM signal power. Resonators 2 and 3 will contribute the most to the PIM signal in a six-cavity filter.

The PIM signals produced by the components result from the conversion of RF energy loss (PIM$\propto P_{Loss}^2$) [11], [12]. The power dissipated by the resistance in resonant circuit P_{Loss} is defined as follows.

$$P_{Loss1} = \frac{1}{2}\frac{|V_1|^2}{R_1}, \qquad P_{Loss2} = \frac{1}{2}\frac{|V_2|^2}{R_2}, \tag{3}$$

where R_1 and R_2 are the resistance of equivalent parallel resonant circuits.

The power loss in the resonant circuit is inversely proportional to the resistance R. To reduce the PIM power in the resonator filter, it would be necessary to reduce the power loss that is proportional to the PIM power in the air cavity filter. Table 1 shows the resistances, maximum voltages, power losses, and relative PIM signal levels of a resonator for various cavity sizes. In this case, the input power was 20 W.

Table 1. The resistances, maximum voltages, power losses, and relative PIM signal levels for air cavity filters of various cavity sizes.

Inner/Outer Radius (mm)	R (kΩ)	$V_{Max.}$ (V)	P_{Loss} (mW)	PIM/PIM(6/18) (dB)
6/12	144.86	432.844	925.88	7.68
6/18	409.38	559.363	382.14	0
6/24	695.31	633.919	164.91	–7.31

In this example, all the PIM signal levels are based on the voltage and resistance in the coaxial resonator structure. The increase of the outer conductor radius carried a larger resistance

and larger voltage at a given power, and the PIM power generated was smaller. The total relative ratios of PIM power were 7.68 dB, 0 dB, and –7.31 dB at b = 12 mm, 18 mm, and 24 mm, respectively. In this example, the reference power level is the PIM power of an air cavity filter made up of cavities with an outer radius b=18 mm, an inner radius a=6 mm, and a 0.01 ripple. We used the same reference power level for the remaining example calculations.

We now consider the linear response of the filters, for example, the bandwidth, insertion loss, ripple, and center frequency for filters of various sizes. Figure 4 shows the insertion loss estimated for various filters (b=12, 18, 24 mm) at an input power of 20 W. The insertion losses, estimated at 935 MHz/960 MHz were –0.78 dB/–0.65 dB, –0.44 dB/–0.37 dB, and –0.33 dB/–0.28 dB with b = 12 mm, 18 mm, and 24 mm, respectively. This means that the PIM signal response and insertion loss response have coherence.

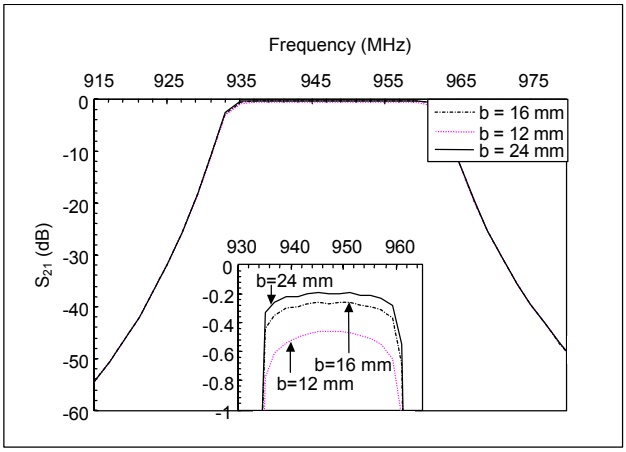

Fig. 4. The insertion loss characteristics of three different types of filters.

For practical applications, it is important to investigate whether the PIM power can be minimized by any means, for example, by adjusting the inner radius of the cavity in the filter when the outer radius is fixed. Figure 5 gives the power loss and relative PIM signal levels for various inner radii of the coaxial air cavity filter.

The resistance and voltage in the coaxial resonator are inversely proportional to the inner radius. The power dissipated in the coaxial resonator structure that makes up a filter has a minimum value in a specific range. The optimized inner size that minimizes the PIM signal of the filters is between 4.8 mm and 5.2 mm. This means that the transmission line impedance Z_0 is 74.5 Ω to 79.3 Ω.

We also wanted to determine whether the PIM power can be reduced by an optimization process that adjusts the filter size without degrading or varying other filter specifications.

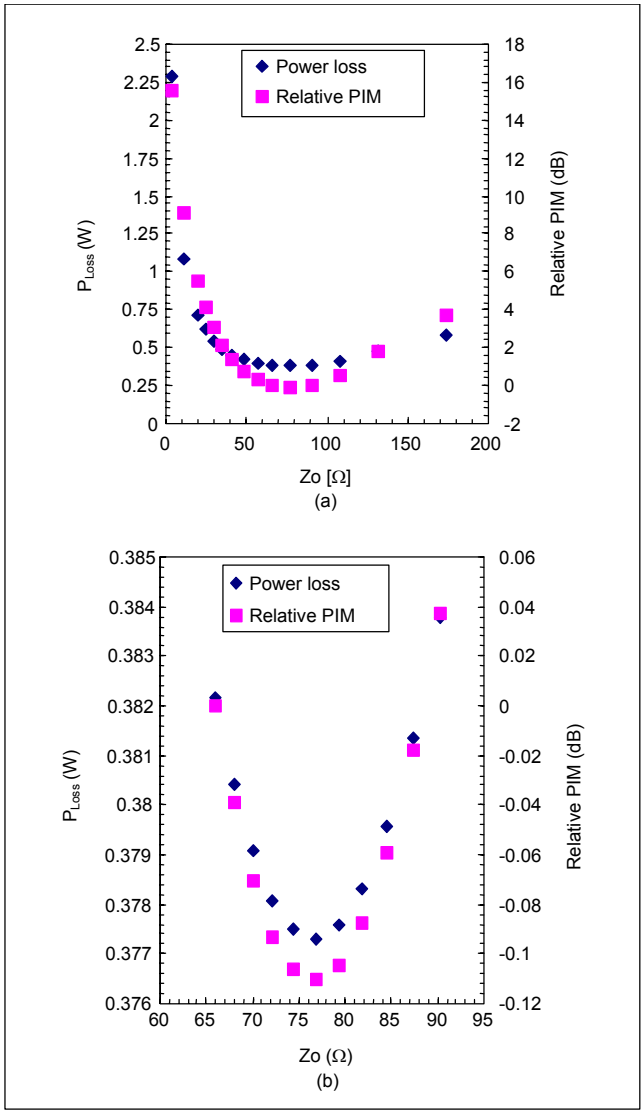

Fig. 5. The power loss and relative PIM signal level versus impedance of the coaxial air cavity filters with different inner radii: (a) wide scale, (b) narrow scale.

Figure 6 shows the variation of the relative PIM signal level, attenuation, and return loss of the filter with its pass band ripple.

Figure 6(a) shows that increasing the ripple of the filter causes an increase of the PIM signal level and the attenuation. This means that an increase of the pass band ripple degrades the PIM performance but improves the attenuation performance. Figure 6(b) shows that a decrease of the pass band ripple improves the return loss in the filter's pass band. These results indicate that the general RF specification might be at odds with a low PIM signal power. Therefore, minimizing the PIM signal power may produce a filter that does not have the required linear filter specifications.

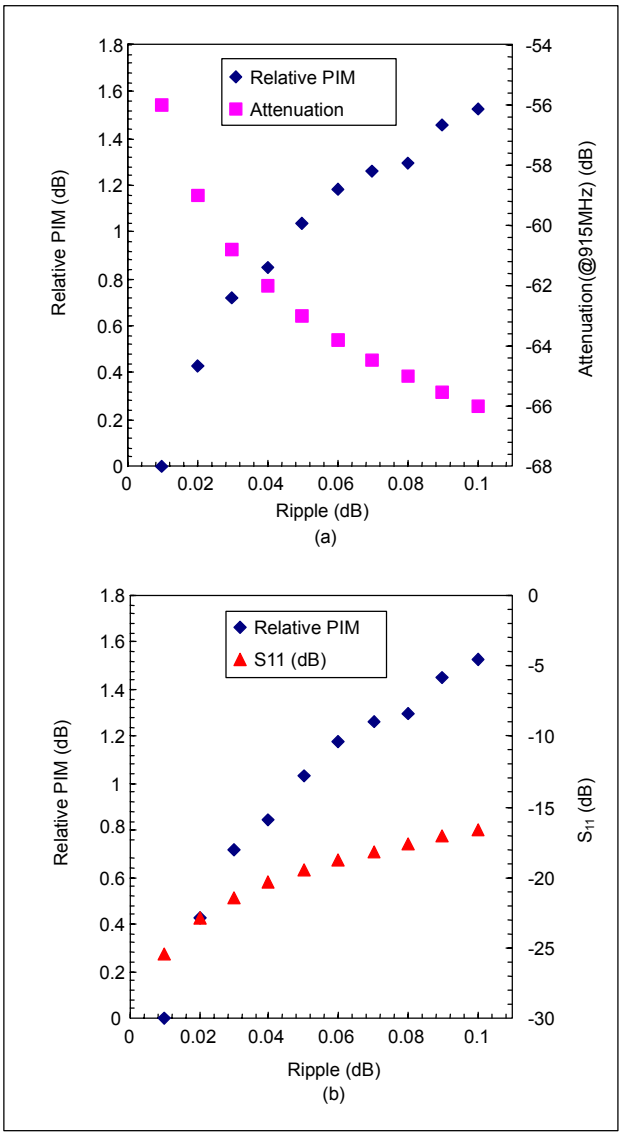

Fig. 6. Variation of the RF and PIM power characteristics of six cavity filters with the pass band ripple:
(a) variation of the relative PIM power values and the attenuation with the pass band ripple,
(b) variation of the relative PIM power values and the return loss values with the pass band ripple.

IV. MEASUREMENT RESULTS AND DISCUSSION

To verify the PIM power assumptions using the power dissipated in the resonators, we manufactured and measured experimental filters. The filters consisted of an aluminum substrate coated with a thin zinc layer and plated with 8 μm thick silver. The design and manufacture of the six-cavity filters is based on the result shown in Table 1. Figure 7 shows the insertion loss within the required frequency range for various outer radius sizes.

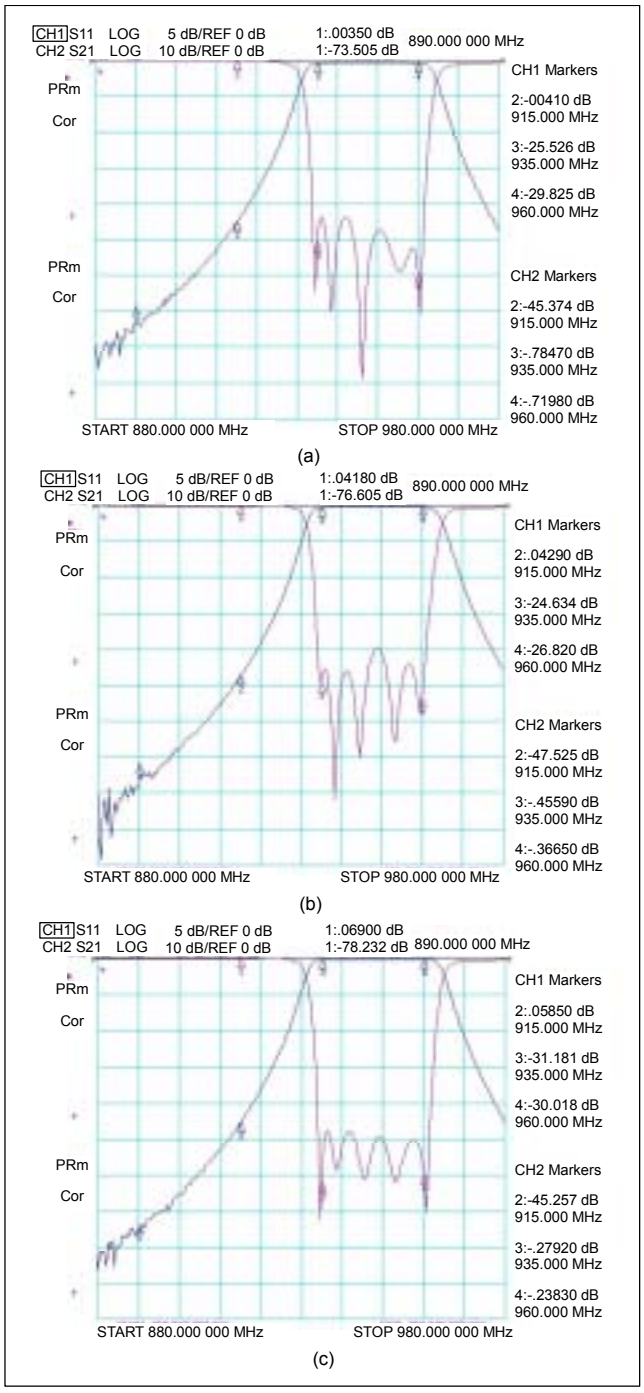

Fig. 7. The measured RF filter characteristics for different outer radius values: (a) b=12 mm, (b) b=18 mm, (c) b=24 mm.

The insertion losses at 935 MHz/960 MHz were –0.78 dB/–0.72 dB, –0.46 dB/–0.37 dB, and –0.28 dB/–0.24 dB at b = 12 mm, 18 mm, and 24 mm, respectively. These results conform to the predictions in Fig. 4. The notable result of the RF measurement is that an increase of the outer radius size reduces the insertion loss in a six-cavity filter.

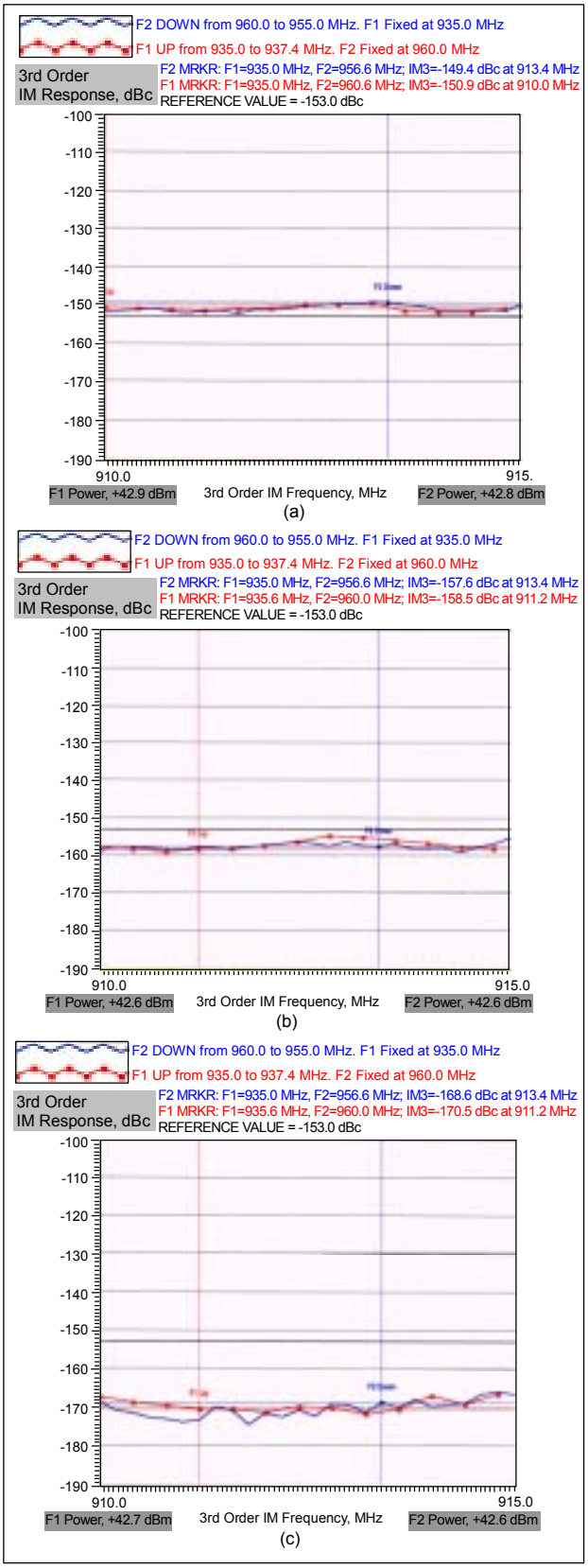

Fig. 8. The measured PIM characteristics of six cavity filters for three different outer radius values: (a) b=12 mm, (b) b=18 mm, (c) b=24 mm.

For the PIM measurements we used a Summitek Instruments' PIM Analyzer (SI-900A), a 1/2 inch coaxial cable assembly, and a 7/16 inch DIN Male to N Male adapter. The PIM levels of these components were below –170 dBc.

Figure 8 shows the PIM measurement results for the manufactured filters.

The average PIM levels of the GSM band were –151.36 dBc, –157.24 dBc, and –169.53 dBc at b = 12 mm, 18 mm, and 24 mm, respectively. Where input powers were 2×43 dBm, we made three measurements with two hours between measurements. The repeatability was ±2 dB and the maximum measurement uncertainty ±1 dB. These results are in agreement with the assumptions in Table 1. We consider the measured results to be very good. Table 2 compares the experimental (Figs. 7 and 8) and theoretical (Table 1 and Fig. 4) results.

Table 2. The comparison between the experimental (Fig. 7, Fig. 8) and theoretical (Table 1, Fig. 4) results.

Inner/Outer Radius (mm)	Theoretical		Experimental	
	Insertion loss (dB) (@935MHz/ 960 MHz)	PIM/PIM 6/18) (dB)	Insertion loss (dB) (@935MHz/ 960 MHz)	PIM/PIM (6/18) (dB)
6/12	–0.78/–0.65	7.68	–0.78/–0.72	5.88
6/18	–0.44/–0.37	0	–0.46/–0.37	0
6/24	–0.33/–0.28	–7.31	–0.28/–0.24	–12.29

We think that the difference between the theoretical and experimental PIM power was caused by the difference of the filter insertion loss. For the 6/12 cavity filter, for example, the relation between the PIM power and insertion loss was obvious (Table 2).

V. CONCLUSIONS

This paper explained how the PIM power arising in an air cavity filter could be calculated. These calculations were used to reduce the level of PIM signals by optimizing the filter cavity sizes. We calculated and measured the PIM power levels of three different sizes of air cavity filters, with cavity outer radii of 12 mm, 18 mm, and 24 mm. We found not only that the cavity's characteristic impedance must be between 74 Ω and 79 Ω to minimize the PIM power in an air cavity filter, but also that the general RF performance under these conditions would not be at its best if it was designed for low PIM power. This showed that our method for optimum design is successful

when the PIM power and other characteristics of the cavity filter are considered.

REFERENCES

[1] B.G.M. Helme, *Passive Intermodulation of ICT Components*, The Institution of Electrical Engineers, 1998.

[2] Byung-Jun Jang, In-Bok Yom, and Seong-Pal Lee, "Millimeter Wave MMIC Low Noise Amplifiers Using a 0.15 μm Commercial pHEMT Process," *ETRI J.*, vol. 24, no. 3, June 2002, pp. 190-196.

[3] G.H. Schennum and G. Rosati, "Minimizing Passive Intermodulation Product Generation in High Power Satellites," *IEEE Proc. of Aerospace Applications Conf.*, vol. 3, 1996, pp. 155-164.

[4] Jin Tae Kim, In-Kui Cho, Myung Yung Jeong, and Tae-Goo Choy, "Effect of External PIM Sources on Antenna PIM Measurements," *ETRI J.*, vol. 24, no. 6, Dec. 2002, pp. 435-442.

[5] P. Bolli, S. Selleri, and G. Pelosi, "Passive Intermodulation on Large Reflector Antennas," *IEEE Antennas and Propagation Magazine*, vol. 44, Oct. 2002, pp.13-20.

[6] F. Arazm and F.A. Benson, "Nonlinearities in Metal Contacts at Microwave Frequencies," *IEEE Trans. on Electromagnetic Compatibility*, vol. EMC-22, no. 3, Aug. 1980, pp. 142-149.

[7] B. Deats and R. Hartman, "Measuring the Passive-IM Performance of RF Cable Assemblies," *Microwave & RF*, Mar. 1997, pp. 108-114.

[8] J.Z. Wilcox and P. Molmud, "Thermal Heating Contribution to Intermodulation Fields in Coaxial Waveguides," *IEEE Trans. on Communications*, Feb. 1976, pp. 238-243.

[9] G.L. Matthaei, L. Young, and E.M. Jones, *Microwave Filters, Impedance Matching Networks and Coupling Structures*, Dedham, MA, Artech, 1980.

[10] J.H. Kim, S.K. Han, K.Y. Kang, and D. Ahn, "Temperature Dependence of Microwave Properties of HTS Multipole Lowpass Filters Consisting of Microstrip Open-Stub Lines," *ETRI J.*, vol. 19, no. 2, July 1997, pp. 48-58.

[11] G.H. Stauss, *Intrinsic Sources of IM Generation*, NRL Memorandum Report 4233, 1980.

[12] G.C. Liang, D. Zhang, and C.F. Shih, "High-Power HTS Microstrip Filters for Wireless Communication," *IEEE Trans. on Microwave Theory and Techniques*, vol. 43, no. 12, Dec. 1995, pp. 3020-3029.

In-Kui Cho was born in Kyungnam, Korea, on April 8, 1970. He received the BS and MS degrees from the Department of Electronic Engineering, Kyungpook National University, Korea, in 1997 and 1999. Since May 1999, he has worked for Electronics and Telecommunications Research Institute (ETRI). Present research interests include Passive Intermodulation (PIM) of RF components, optical interconnection, signal integrity, and interconnect modeling.

Jin Tae Kim received his BS degree in physics from the University of Incheon in 1996 and his MS from Korea University in 1998. His main research was on NMR/MRI and he worked in Asan Medical Center, Seoul, Korea, in 2000. In October 2000, he joined Electronics and Telecommunications Research Institute (ETRI), Daejeon, Korea, where he worked on the Passive Intermodulation (PIM) in mobile telecommunication components. Since 2002, he has investigated a polymeric waveguide device based on LIGA and MEMS.

Myung Yung Jeong was born in Kyungnam, Korea, on February 20, 1960. He received the BS and MS degrees from Pusan National University, Korea, in 1982 and 1984 and the PhD degree from Korea Advanced Institute of Science and Technology, Korea, in 2000. Since September 1983, he has worked for Electronics and Telecommunications Research Institute (ETRI). Present research interests include hot embossed optical devices, photonic crystals, optical interconnection, and packaging. He is now the Team Leader of the Optical Interconnection Team, ETRI.

Tae-Goo Choy received the BS and MS degrees in physics from Korea University in 1972 and 1976. He joined the Component Technology Development Section at ETRI in 1977, where he is currently the Head of Section. He is interested in microwave and optical components. He holds 15 patents and has authored over 40 papers.

Young Il Kang started his professional carrier at Fairchild Semiconductor (Korea) in 1969 and serviced as a product engineer until he moved to ETRI in 1979. He developed the wafer fabrication process for 32k/64k PROM at the early stage of ETRI and has continued his work for the development of various ICs for the telecommunication industry. His educational background consists of a BS degree in electrical engineering from the Seoul National University in 1966, an MS degree in electrical engineering from the Fairleigh Dickinson University in 1991, and a PhD degree of computer science from Korea University in 1996.